International Global Navigation Satellite Systems Society
IGNSS Symposium 2015

Outrigger Gold Coast, Qld Australia
14-16 July, 2015

Performance Analysis of AOA-based Localization with Software Defined Radio

Donggu Kim
Department of Electrical Engineering
Korea Advanced Institute of Science and Technology (KAIST), Korea
Phone +82-42-350-7522 Fax +82-42-350-7622, kdg26@kaist.ac.kr
Seongah Jeong
Department of Electrical Engineering
Korea Advanced Institute of Science and Technology (KAIST), Korea
Phone +82-42-350-7522 Fax +82-42-350-7622, seongah@kaist.ac.kr
Kwang Eog Lee
Agency for Defense Development (ADD), Korea
Phone +82-42-821-2136, kelee@add.re.kr
Joonhyuk Kang
Department of Electrical Engineering
Korea Advanced Institute of Science and Technology (KAIST), Korea
Phone +82-42-350-7422 Fax +82-42-350-7622, jhkang@ee.kaist.ac.kr

ABSTRACT

In this paper, we investigate angle of arrival (AOA)-based estimation of a mobile station (MS)'s location by monitoring the AOA at multiple reference software defined radio (SDR) receivers. Each Universal software radio peripheral (USRP) device captures the AOA from the uplink transmission of a MS via MUltiple SIgnal Classification (MUSIC), which is one of super-resolution techniques to estimate AOA by using pseudo-spectrum. Subsequently, two-dimensional (2D) angulation is adopted for locating the MS based on AOA measurements and references' positions. We consider the various communication environments, such as i) outdoor area without obstacles, ii) outdoor area with only a few obstacles and iii) indoor area with many obstacles. In order to evaluate the performance of AOA-based localization, we evaluate and compare the mean-squared position error. Via experimental results, an impact of multipath on localization accuracy is verified.

KEYWORDS: Angle of arrival (AOA); MUltiple SIgnal Classification (MUSIC); Two-dimensional (2D) angulation; Universal Software Radio Peripheral (USRP)

1. INTRODUCTION

Location-awareness becomes an interesting issue due to the increase of demand for location-based services (LBS) applications in diverse areas such as emergency response, security, monitoring and location-based commerce (L-commerce) (K. Pahlavan *et al*, 2002, and G. Yanying *et al*, 2009). In general, the Global Navigation Satellite System (GNSS), e.g., Global Positioning System (GPS), provides the precise positioning information with global coverage in outdoor environments (C. J. Hegarty *et al*, 2008). However, the performance of the GPS can be unsatisfactorily degraded in indoor or dense urban area, where GPS signals are interrupted by buildings or enclosed structure. Therefore, the network-based localization using the direction or/and distance information has been developed in order to determine the target's position in GPS-denied area (K. Pahlavan *et al*, 2002, S. Jeong *et al*, 2014, and S. Gezici *et al*, 2005). In network-based localization, angle of arrival (AOA) (S. Gezici *et al*, 2005), time of arrival (TOA) (I. Guvenc *et al*, 2009, Y. Shen *et al*, 2014, and T. Wang *et al*, 2014), time difference of arrival (TDOA) (M. Aatique, 1997), and received signal strength (RSS) approaches can be utilized to estimate the position of target, e.g., a mobile station (MS), by using the radio frequency (RF) signal, received at the multiple reference nodes, e.g., base stations (BS).

The AOA-based localization can determine the two-dimensional (2D) location with only two reference nodes while the distance-based localization using TOA, TDOA, or RSS needs at least three reference nodes (J. Hightower *et al*, 2001). Furthermore, AOA-based localization does not require the synchronization process between the MSs and multiple reference nodes. For these reasons, AOA-based localization can be considered as a practical approach in real-world applications (J. Ni *et al*, 2006).

In this paper, we study and analyze the AOA-based localization with Universal Software Radio Peripheral (USRP) (U. Pesovic *et al*, 2012, and T. S. Clinci *et al*, 2013), which is the well-known software defined radio (SDR) platforms. We consider the uplink scenario, where the multiple reference nodes with multiple antennas perform the uplink positioning to locate a single MS in 2D region. Specifically, based on the AOA measurements achieved at the different two reference nodes using USRPs and via the Multiple Signal Classification (MUSIC) algorithm (T. Lavate *et al*, 2010), we perform the 2D angulation geometrically for finding the MS. For the verification of an impact of multipath on the localization accuracy, the mean-squared position errors is adopted and evaluated in the various communication environments. In the experimental results, although it is observed that the accuracy of the estimated AOA and thus the MS's position decreases due to the multipath effect, the acquired mean-squared position errors are relatively small with regard to the inter-node distance between the MS and the reference nodes. Accordingly, we can expect the reliable performance of the AOA-based localization in multipath environments.

The rest of the paper is organized as follows. Section 2 presents the AOA-based localization technique using MUSIC and 2D angulation. In Section 3 and Section 4, the experimental setup and results are provided, respectively. Finally, this paper is concluded in Section 5.

2. AOA-BASED LOCALIZATION

In this section, we cover the AOA-based localization using MUSIC algorithm and 2D angulation.

2.1 MUltiple SIgnal Classification (MUSIC)

MUSIC is one of the popular super-resolution techniques to estimate the AOA by measuring the pseudo-spectrum. In particular, we consider M signals impinging on a uniform linear array (ULA) with N antennas, which are half-a-wavelength apart. The received signal at ULA can be expressed as:

$$\mathbf{x} = \sum_{m=1}^{M} \alpha_m \mathbf{s}(\phi_m) + \mathbf{n}, \tag{1}$$

where α_m represents the complex attenuation of the m-th waves; $\mathbf{s}(\phi_m)$ denotes the steering vector of the signal, whose direction is denoted as ϕ_m; and $\mathbf{n}$ is the additive white Gaussian noise (AWGN) with zero mean and the variance σ^2. In matrix notation, (1) becomes

$$\mathbf{x} = \mathbf{S}\boldsymbol{\alpha} + \mathbf{n}, \tag{2}$$

where

$$\mathbf{S} = [\mathbf{s}(\phi_1), \mathbf{s}(\phi_2), \ldots, \mathbf{s}(\phi_M)] \tag{3}$$

denotes the $N \times M$ steering matrix and

$$\boldsymbol{\alpha} = [\alpha_1, \alpha_2, \ldots, \alpha_M]^T \tag{4}$$

denotes the $M \times 1$ complex signal vector. Assuming that the different complex signals to be uncorrelated, the covariance matrix of the received signal $\mathbf{x}$ can be given as:

$$\begin{aligned} \mathbf{R} &= \mathrm{E}\left[\mathbf{x}\mathbf{x}^H\right], \\ &= \mathrm{E}\left[\mathbf{S}\boldsymbol{\alpha}\boldsymbol{\alpha}^H\mathbf{S}^H\right] + \mathrm{E}\left[\mathbf{n}\mathbf{n}^H\right], \\ &= \mathbf{S}\mathbf{A}\mathbf{S}^H + \sigma^2\mathbf{I}, \\ &= \mathbf{R}_s + \sigma^2\mathbf{I}, \end{aligned} \tag{5}$$

where the signal covariance matrix $\mathbf{R}_s$ is a $N \times N$ matrix with having the $N - M$ eigenvectors corresponding to the smallest eigenvalues. The noise subspace $\mathbf{Q}_n$, which is the $N \times (N - M)$ matrix consisting of such $N - M$ eigenvectors, is orthogonal to M steering vectors of the signals. By using the orthogonal property between the noise and signal subspaces, MUSIC pseudo-spectrum provides the accurate AOA measurements, which is defined as

$$P_{MUSIC}(\phi) = \frac{1}{\mathbf{s}^H(\phi)\mathbf{Q}_n\mathbf{Q}_n^H\mathbf{s}(\phi)}. \tag{6}$$

Note that the denominator of (6) converges to zero when ϕ become closer to the actual AOA, and thus MUSIC pseudo-spectrum $P_{MUSIC}(\phi)$ has the M peaks corresponding to the M signal directions.

2.2 Two-dimensional (2D) Angulation

The location of the MS can be determined by the angle measurements at the two reference nodes, whose positions are known in advance. Fig. 1 shows the diagram of 2D angulation to locate the single MS in X-Y coordinate plane. We denote the two reference nodes' positions as (x_1, y_1) and (x_2, y_2), respectively. The reference node 1 and 2 estimate the inter-node angle α_1

and α_2 via MUSIC algorithm discussed in previous section.

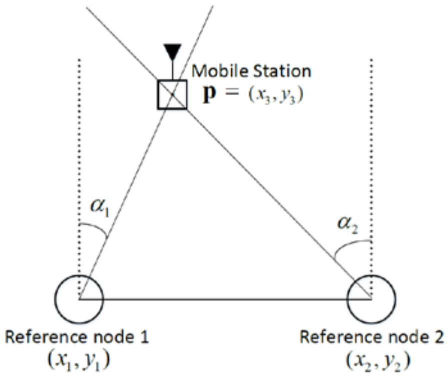

Figure 1. Diagram of 2D angulation based on X-Y coordinate plane

Based on the captured AOA and reference nodes' positions, the location of MS can be finally determined as:

$$x_3 = \frac{y_1 - y_2 + \dfrac{x_1}{\tan\alpha_1} + \dfrac{x_2}{\tan\alpha_2}}{\dfrac{1}{\tan\alpha_1} + \dfrac{1}{\tan\alpha_2}}, \tag{7}$$

and

$$y_3 = y_1 - \frac{1}{\tan\alpha_1}\left(x_1 - \frac{y_1 - y_2 + \dfrac{x_1}{\tan\alpha_1} + \dfrac{x_2}{\tan\alpha_2}}{\dfrac{1}{\tan\alpha_1} + \dfrac{1}{\tan\alpha_2}} \right). \tag{8}$$

3. EXPERIMENTAL SETUP

In this section, we first show the overall configuration of the AOA-based localization system with SDR platform and experimental setup for USRPs, and then, in the various communication scenarios such as i) outdoor area without obstacles, ii) outdoor area with only a few obstacles and iii) indoor area with many obstacles, we analyze the mean-squared position error of the estimated position achieved by 2D angulation.

3.1 AOA-based Localization System Configuration

For the performance analysis, we consider the AOA estimation system, which is composed of National Instruments (NI) USRP-2921 with two transceiver ports given as TX1/RX1 and TX2/RX2, respectively (NI, 2015). Also, 2.4 GHz omnidirectional vertical antennas and LabView software are included in this estimation system. Generally, the AOA estimation utilizes the phase difference of the received signal at each antenna of the array, which is given in the steering vector as in (3). For the frequency synchronization among the receive antennas by calibrating the phase offset, the external 10 MHz clock with 1 PPS are connected to the USRP receivers and the additional RF reference transmit signal is used to eliminate the phase and gain uncertainty among the Rx USRPs.

Fig. 2 illustrates the overall AOA-based localization system configuration diagram. The omnidirectional vertical antennas are connected to 1 Tx USRP and 4 Rx USRPs using TX1/RX1 port. Due to the use of 2.4 GHz carrier frequency in this experiment, 4 Rx antennas are set to be about 6cm apart. As mentioned before, the external clock equipped with 'Ref in/PPS in' is linked with 4 Rx USRPs using both clock distributor and PPS distributor. For calibration among the received signals, the reference Tx USRP should be connected to the TX2/RX2 of 4 Rx USRPs via 4-way power splitter. On the other hand, in order to exploit the LabView software by using host computer, all of the 6 USRPs and host computer are directly connected to the Gigabit Ethernet Switch with several cables.

By the MUSIC algorithm discussed in Section 2.1, we have designed the appropriate LabView block diagram for Tx signal, Reference Tx signal, and Rx antenna array. In order to improve the reliability of AOA estimation, the MUSIC algorithm in LabView has been designed to collect 10^6 snapshots, and then we calculate the average covariance matrix $\mathbf{R}$ in (5). The details of the experimental setup for USRPs are presented in Table 1.

With the captured AOAs, we finally perform the positioning via 2D angulation method. By substituting both known positions of reference nodes and captured AOAs into (7) and (8), the MS's position can be obtained.

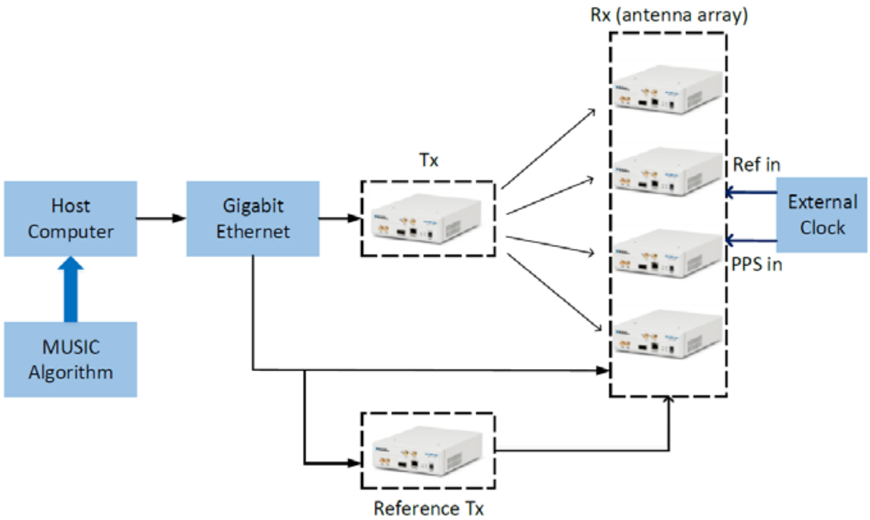

Figure 2. AOA-based localization system configuration

	Tx signal	Reference Tx signal	Rx (antenna array)
Carrier frequency	2.4 GHz	2.4 GHz	2.4 GHz
Sampling rate	1 MHz	1 MHz	1 MHz
Tone frequency	100 KHz	10 KHz	-
Gain	20	20	30

Table 1. Experimental setup for USRPs

3.2 Experimental Environment

In order to evaluate the performance of the localization by using 2D angulation, we consider three different communication environments such as i) outdoor area without obstacles, ii) outdoor area with only a few obstacles and iii) indoor area with many obstacles. Since the localization with 2D angulation requires only two reference nodes, we placed the two reference nodes (i.e., Rx antenna array) at (0,0) and (0.9,0) (m), respectively. Also, the position of the single MS (i.e., Tx of the uplink transmission) is set to be (0.3, 3.3) (m). Fig. 3 describes the positions of all the reference nodes and MS in this experiment. Here, we assume that the far-field condition can be valid, and therefore the arrived signals can be considered as plane waves at the reference nodes.

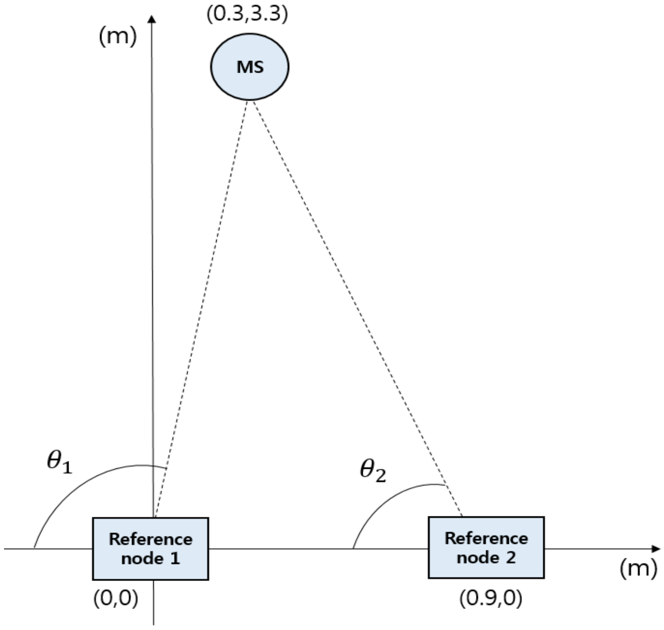

Figure 3. Positions of the reference nodes and MS

Fig. 4 shows the three different experimental environments in Korea Advanced Institute of Science and Technology (KAIST); (a) playground regarded as outdoor area without obstacles, (b) building entrance regarded as outdoor area with a few obstacles such as outer walls of building and (c) laboratory regarded as indoor area with many obstacles. In Fig. 4 (a), it is expected that the localization can be conducted without multipath effect. For Fig. 4 (b), Tx signal can be reflected by the obstacles along the propagation path. Finally, in Fig. 4 (c) with having the relatively many obstacles compared to outdoor scenarios, the localization performance can be expected to be worse than those of outdoor scenarios.

(a)

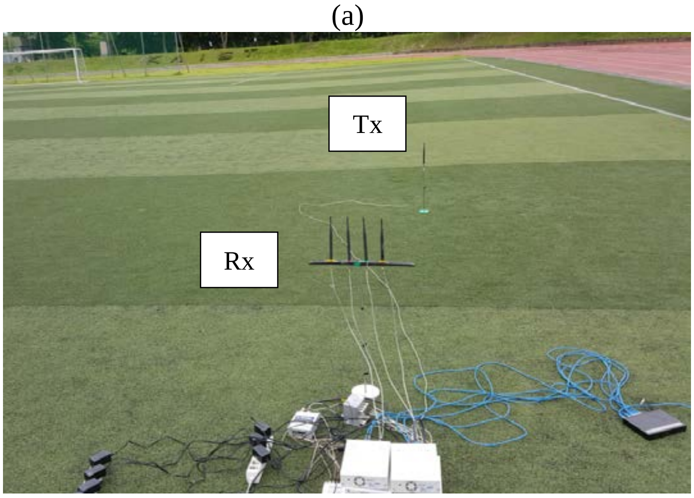

(b)

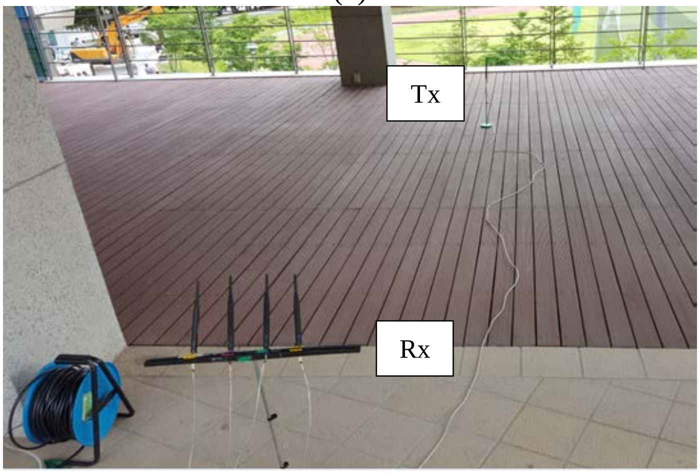

(c)

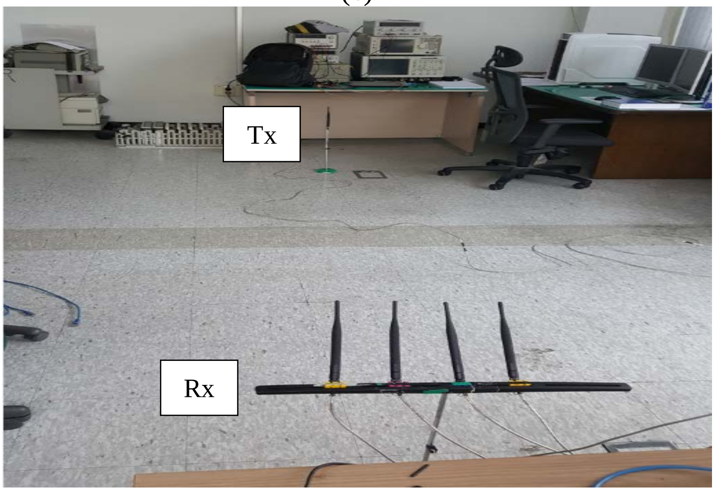

Figure 4. Three different communication environments (a) Outdoor area without obstacles (b) Outdoor area with obstacles (c) Indoor area with obstacles

4. ANALYSIS OF RESULTS

In the following, we provide the corresponding snapshots of the MUSIC pseudo-spectrum for the three scenarios, such as i) outdoor area without obstacles, ii) outdoor area with only a few obstacles and iii) indoor area with many obstacles in Fig. 5, 6 and 7, respectively. The actual AOA θ_1 and θ_2 described in Fig. 3 are 95.2° and 79.7°, respectively. In scenario i), outdoor area without obstacles, the estimated AOA at reference node 1 and 2 are 95° and 79.5°, respectively, which are the closest to the actual AOA among three conditions. In outdoor with a few obstacles, it is seen that the estimated AOA at reference node 1 and 2 are 96° and 78°, respectively. This can be explained by the fact that a few obstacles degrade the performance of the AOA measurement. Similarly, we notice that the accuracy of AOA measurement significantly decreases in indoor area to 98.5° and 75° as depicted in Fig. 7 due to many obstacles compared to the previous two scenarios.

(a)

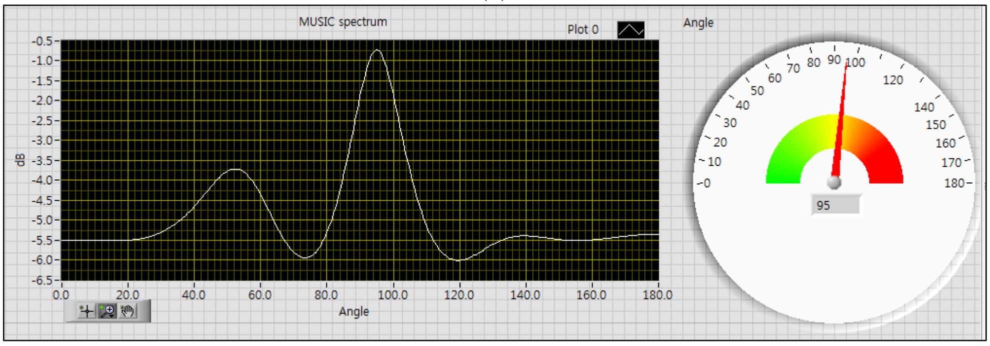

(b)

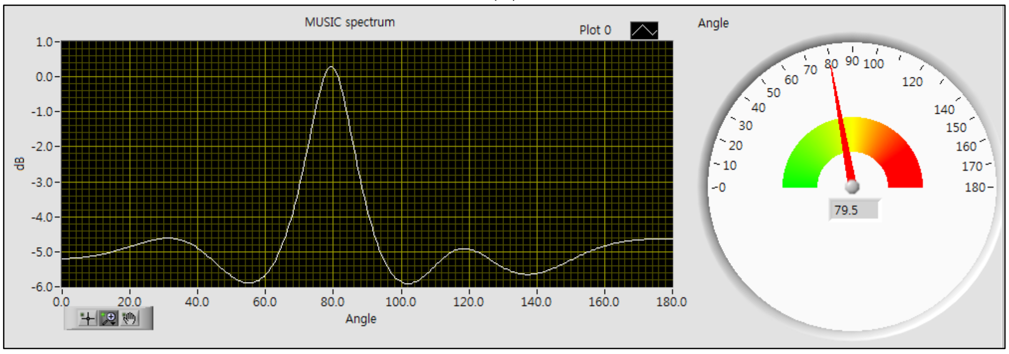

Figure 5. MUSIC spectrum and estimated AOA in outdoor area without obstacles
(a) Estimated AOA at reference 1: 95° (b) Estimated AOA at reference 2: 79.5°

(a)

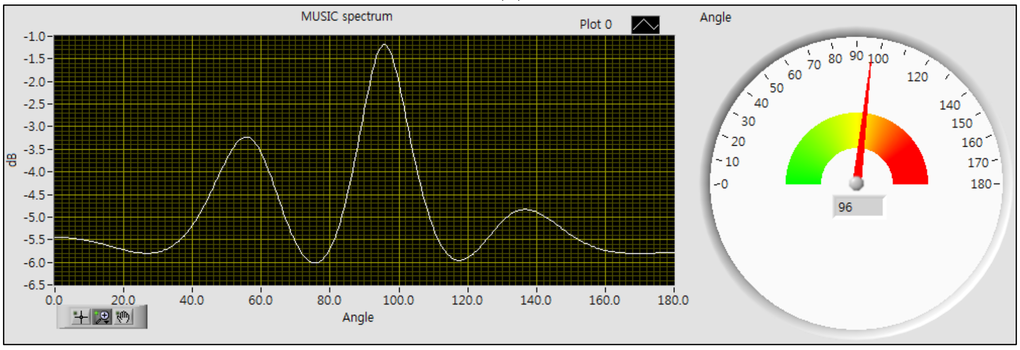

(b)

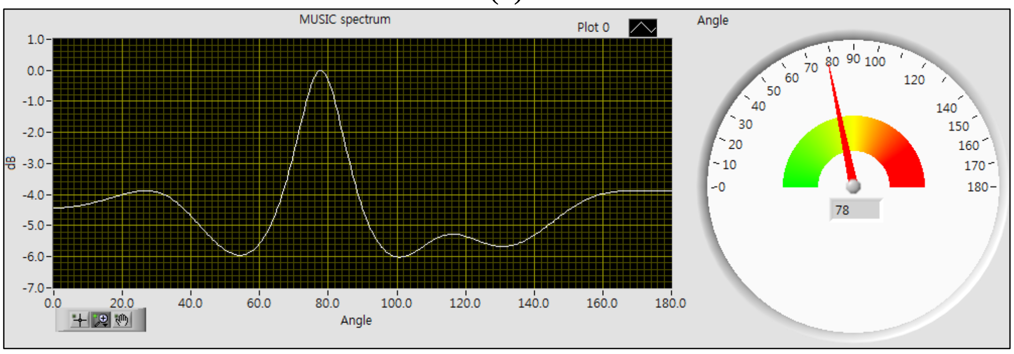

Figure 6. MUSIC spectrum and estimated AOA in outdoor area with obstacles
(a) Estimated AOA at reference 1: 96° (b) Estimated AOA at reference 2: 78°

(a)

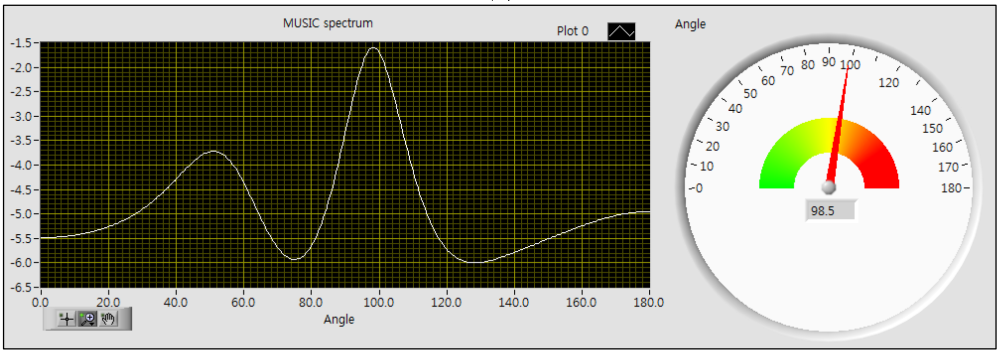

(b)

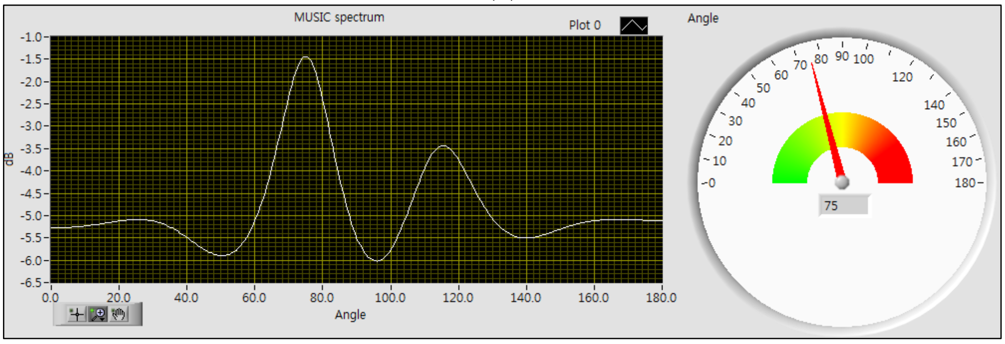

Figure 7. MUSIC spectrum and estimated AOA in indoor area with obstacles
(a) Estimated AOA at reference 1: 98.5° (b) Estimated AOA at reference 2: 75°

By using the AOA obtained in Fig. 5 to Fig. 7, we estimate the location of the MS based on 2D angulation given as (7) and (8). From Fig. 8 to Fig. 10, we present the final positions estimated by the 2D angulation in three experiment scenarios. We investigate the 20 estimated locations of the MS for each experiment in order to evaluate the performance of the considered AOA-based localization system. In Fig. 8, the estimated positions of the MS in outdoor area without obstacles are given. Since the almost multipath free environment can be guaranteed, it is shown that the most of the estimated positions are distributed near the actual position. However, when the obstacles are present, the estimated positions become far from the actual position of the MS as shown in Fig. 9 and 10, which implies that the localization accuracy is deteriorated by the multipath effects.

Moreover, in order to evaluate and compare the localization accuracy mathematically, the mean-squared position error is adopted (S. Jeong *et al*, 2014) and given as

$$\rho = E\left[\left\|\hat{\mathbf{p}} - \mathbf{p}\right\|^2\right], \tag{9}$$

where $\hat{\mathbf{p}}$ denotes the estimated location of MS given as $\hat{\mathbf{p}} = (\widehat{x_3}, \widehat{y_3})$. Note that since the mean-squared position error ρ is the variance of the positioning error, the smaller value of ρ implies the higher localization accuracy. The values of ρ achieved from the experiments are also presented in Fig. 8 to 10. For three scenarios, the values of ρ is given as i) $\rho_1 = 0.0281$; ii) $\rho_2 = 0.2271$; and iii) $\rho_3 = 0.6004$. In terms of the mean-squared position error ρ, we can verify the impact of multipath on the localization accuracy.

In spite of the multipath effects, all of the computed mean-squared position errors can be acceptable, comparing to the distances between the MS and the reference node given by $d = 3.3541$ (m) in Fig. 8. In order to examine the feasibility of 2D angulation with SDR platform, we consider the worst-case among three scenarios, namely, indoor area where the values of $\sqrt{\rho_3}$ is 0.7748 (m), which is about 23% of d. Throughout the experimental results, it can be expected that the reliable performance of the AOA-based localization can be achieved with the SDR platform even in multipath environments.

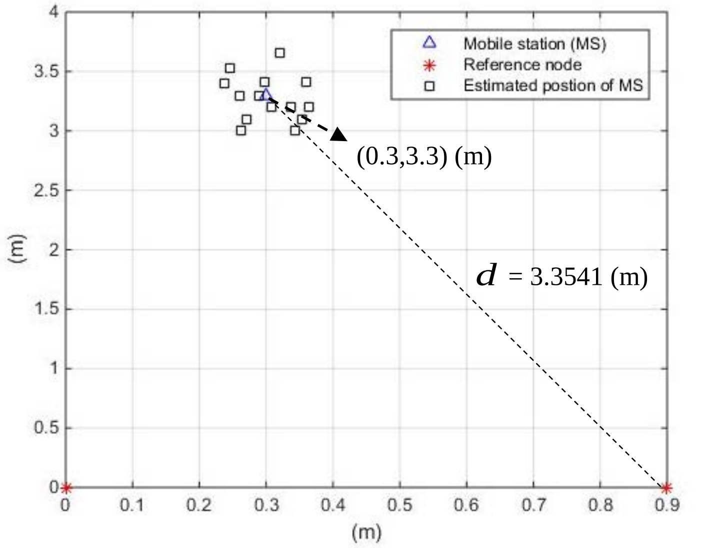

Mean-squared position error $\rho_1 = 0.0281$

Figure 8. Results of AOA-based localization in outdoor area without obstacles

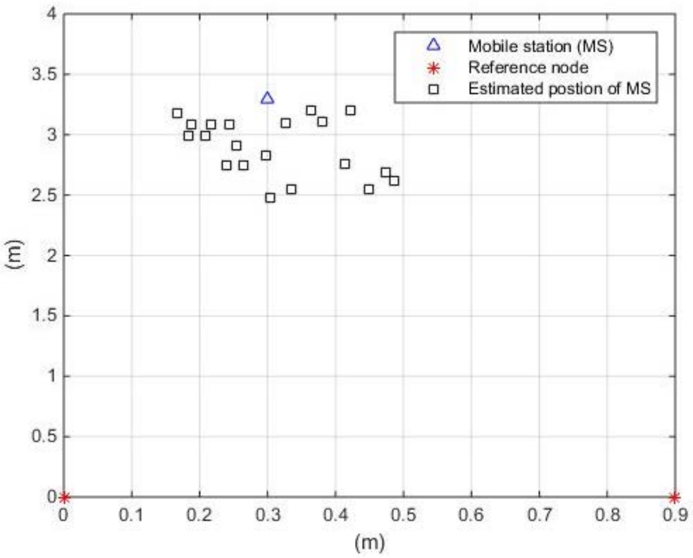

Mean-squared position error $\rho_2 = 0.2271$

Figure 9. Results of AOA-based localization in outdoor area with obstacles

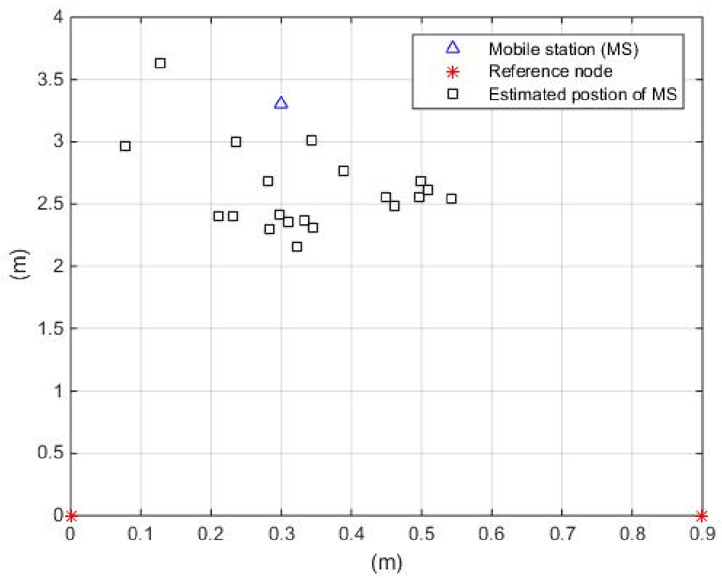

Mean-squared position error $\rho_3 = 0.6004$

Figure 10. Results of AOA-based localization in indoor area with obstacles

5. CONCLUDING REMARKS

In this paper, we have studied the performance analysis of AOA-based localization using USRPs and LabView software. In order to measure AOA, the conventional MUSIC algorithm is applied for LabView design. Particularly, focusing on the impact of multipath on localization accuracy, the various experiment scenarios are considered. In experimental results, it is observed that the severe multipath in indoor area and by the obstacles significantly degrades the localization accuracy. Additionally, we verify that the 2D angulation based on observed AOA by using SDR platform can provide the reliable localization accuracy in terms of the mean-squared position error.

ACKNOWLEDGEMENTS

This work has been supported by the National GNSS Research Center program of Defense Acquisition Program Administration and Agency for Defense Development.

REFERENCES

K.Pahlavan, X. Li, and J.-P. Makela (2002) Indoor geolocation science and technology, *IEEE Commun. Magazine*, vol. 40, no. 2, pp. 112-118, Feb. 2002

G. Yanying, A. Lo, and L. Niemegeers (2009) A survey of indoor positioning systems for wireless personal networks, *IEEE Communications Surveys & Tutorials*, vol. 11, no. 1, pp. 13-32, 2009

C. J. Hegarty, and E. Chatre (2008) Evolution of the Global Navigation Satellite System (GNSS), *Proc. IEEE*, vol. 96, no. 12, pp. 1902-1917, Dec. 2008

S. Jeong, O. Simeone, A. Haimovich, and J. Kang (2014) Beamforming design for joint localization and data transmission in distributed antenna system, *IEEE Trans. on Veh. Technol*., vol. 64, no. 1, pp. 62-76, Apr. 2014

S. Gezici, Z. Tian, G. B. Giannakis, H. Kobayashi, A. F. Molisch, H. V. Poor, and Z. Sahinoglu (2005) Localization via ultra-wideband radios: a look at positioning aspects for future sensor networks, IEEE Signal Proc. Magazine, vol. 22, no. 4, pp. 70-84, July 2005

I. Guvenc, and C.-C. Chong (2009) A survey on TOA based wireless localization and NLOS mitigation techniques, *IEEE Commun. Surveys & Tutorials*, vol. 11, no. 3, pp. 107-124, 3rd Quarter 2009

Y. Shen, W. Dai, and M. Z. Win (2014) Power optimization for network localization, *IEEE/ACM Trans. on Networking*, vol. 22, no. 4, pp. 1337-1350, Aug. 2014

T. Wang, Y. Shen, S. Mazuelas, H. Shin, and M. Z. Win (2014) On OFDM ranging accuracy in multipath channels, *IEEE Syst. J.*, vol. 8, no. 1, pp. 104-114, Mar. 2014

M. Aatique (1997) Evaluation of TDOA techniques for position location in CDMA systems, *Ph.D. dissertation*, Virginia Polytechnic Inst. State Univ., Blacksburg, VA, USA, 1997

J. Hightower, and G. Borriello (2001) Location sensing techniques, *Technical Report UW CSE* 2001-07-30, Department of Computer Science and Engineering, University of Washington, 2001

J. Ni, D. Arndt, P. Ngo, C. Phan, and J. Gross (2006) Ultra-wideband two-cluster tracking system design with angle of arrival algorithm, in *Proc. IEEE Conference on Radar*, vol. 6, pp. 24-27, Apr. 2006

U. Pesovic, D. Gliech, P. Planinsiz, Z. Stamenkovic, and S. Randic (2012) Implementation of IEEE 802.15.4 transceiver on software defined radio platform, in *20th Telecommunications Forum (TELFOR '12)*, Belgrade, Serbia, Nov. 2012

T. S. Clinci, and P. I. Dragomir (2013) Perspectives for development of new positioning systems, *Recent Advances in Geodesy and Geomatics Engineering - Proceedings of the 1st European Conference of Geodesy & Geomatics Engineering (GENG '13)*, Antalya, Turkey, pp. 190-197, Oct. 2013

T. Lavate, V. Kokate, and A. Sapkal (2010) Performance analysis of MUSIC and ESPRIT DoA estimation algorithms for adaptive array smart antenna in mobile communication, *International Journal of Computer Networks (IJCN)*, vol. 2, no. 3, pp. 152-172, Jul. 2010

National Instruments (NI) Data-sheet, NI USRP-2921, http://www.ni.com, Feb. 2015